Quantitative laser mass spectroscopy of sputtered versus evaporated metal atoms

Eftihia Varoucha, Nektarios A. Papadogiannis, and Dimitrios Charalambidis
Foundation for Research and Technology–Hellas, Institute of Electronic Structure and Laser, Laser and Applications Division, P.O. Box 1527, GR-711 10 Heraklion, Greece
and Department of Physics, University of Crete, P.O. Box 2208, GR-710 03 Heraklion, Greece

Alejandro Saenz
Fachbereich Chemie, Universität Konstanz, Fach M 721, D-78457 Konstanz, Germany

Hartmut Schröder
Max-Planck-Institut für Quantenoptik, P.O. Box 1513, D-85740 Garching, Germany

Bernd Witzel
Department of Molecular and Optical Physics, Stephan-Meier Straße 19, 79104 Freiburg, Germany
(Received 26 June 2001; published 11 December 2001)

We demonstrate that the presence of excited states in sputtered surface atoms after ion bombardment affects the measured ion yield of a subsequent post multiphoton-ionization processes. This effect was investigated using an advanced time-of-flight mass-spectroscopic technique. This work reports a comparison of two-photon ionization spectra of metallic atoms obtained from solid samples via sputtering and thermal evaporation that reveals the role of excited states. Furthermore we experimentally determine the cross sections for the two photon ionization processes of evaporated Mg, Zn, and In through quantitative ion yield measurement. Numerical configuration interaction calculations for Mg and Zn are presented and the resulting theoretical two-photon ionization cross sections are compared with the measured ones.

DOI: 10.1103/PhysRevA.65.012901 PACS number(s): 79.20.Rf, 32.80.Rm

INTRODUCTION

When an atom is exposed to a strong electromagnetic field, it may undergo one- or multiphoton ionization (MPI) [1]. In the latter case the atomic system is brought from the ground state into an ionic continuum through the simultaneous absorption of more than one photon. In the MPI case, resonant or nonresonant ionization schemes can be encountered, depending on the atomic states and the spectral parameters of the radiation used. MPI combined with mass spectroscopy, also known as laser mass spectroscopy (LMS), has been extensively used for the investigation of the process but also for analytical purposes. Excluding gaseous substances (e.g., rare gas atoms), or materials with low evaporation pressure at room temperature, like a variety of organic substances or mercury, the study of MPI consists of two independent steps, namely (1) ''atomizing'' a solid target by a particle beam and, (2) postionization of the ''atomized'' neutral particles by a laser. For the ''atomization'' of solid samples thermal evaporation, laser ablation, or sputtering can be used. The latter technique is generally known as L-SNMS (laser-secondary neutral mass spectroscopy) [2] or SALI (surface analysis by laser ionization) [3]; for a resonant scheme one also encounters the acronym RIMS [4], which stands for resonance ionization mass spectrometry.

Quantitative ion mass spectroscopy subsequent to MPI allows the identification of the ionization process as a resonant or nonresonant one, as well as the determination of the ionization saturation intensity and generalized cross section. Furthermore it is a valuable tool for quantitative elemental analysis. Quantification of experiments employing MPI involves complications arising from the nonlinear character of the ionization process and from the three-dimensional intensity distribution around the focus of the ionizing laser beam. Because of this intensity distribution and the nonlinearity of the process, the ionization rate is strongly position dependent. As a result, measured spectra usually include what is called volume effects [5]. One has then to account for these volume effects in standard techniques for analyzing measured intensity-dependent ion yields like in the complete comparison method [6,7]. An advanced mass spectroscopic technique that detects only ions originating from a small two-dimensional fixed spatial volume (ISS) [8] in combination with a convolution technique [9] overcomes this problem. This method can be used for ion-yield measurements as well as energy measurements of photoelectrons. In our experiment a three dimensional [3,10–12] fixed spatial volume is used, in which the intensity distribution of the radiation is practically constant. This technique completely eliminates the volume effect complications and permits quantitative studies without any analytical mathematical reconstruction. Such analytical reconstructions are valid only for Gaussian beams and mass spectrometers with no lateral limitations [13]. Realistic reconstructions for any beam profiles and type of lenses are possible only through numerical approaches [6]. A large number of metal atoms, sputtered from metallic targets, have recently been investigated with respect to the type of ionization (resonant, nonresonant), ionization saturation intensities and cross sections, utilizing this technique [14,15]. In these investigations it has been assumed that the majority of the sputtered atoms are in their ground state at the moment they undergo ionization [16]. This assumption is

in general valid [16], but can be violated in certain cases. Since in some of the earlier measurements [14,15] the degree of nonlinearity of the process was found different than the expected one, the need for more detailed investigation of the presence of excited states created during the sputtering process becomes apparent.

In the present work we attempt an investigation of the possible degree of excitation of atoms that are erased from a surface via sputtering and how these states affect the result of multiphoton-ionization spectra and thus the conclusions derived from laser mass spectroscopy. The investigation is based on the comparison of ''two-photon''-ionization spectra of metallic atoms obtained from solid samples via sputtering and thermal evaporation.

For all the elements studied, we extract generalized two-photon ionization saturation intensities and cross sections. The saturation intensities and generalized cross sections are extracted through fitting of known functions to the measured relative ion yields as a function of the ionizing laser intensity. For Mg and Zn, generalized two-photon ionization cross sections have been calculated in a full configuration interaction (CI) calculation performed for the two valence electrons, including core polarization effects. Comparison between measured and calculated cross sections is found satisfactory.

EXPERIMENT

The present experiments combine subpicosecond laser postionization techniques of sputtered or evaporated metal atoms with a time-of-flight (TOF) mass spectroscopic method that permits the registration of ions originating exclusively from the so-called confined interaction volume [10–12]. In this work it has rectangular dimensions of 1800 μm (along the laser propagation direction)$\times$230 μm (along the spectrometer axis)$\times$220 μm (volume $V=9.1\times10^{-5}\,\mathrm{cm}^3$). With this powerful combination, precise measurements of the intensity dependence of ion yields that are free of volume effects have been performed.

The laser system [17,18] employed is a hybrid seven-dye double-excimer laser system, producing pulses at a repetition rate of 5 Hz and with maximum pulse energy of 14 mJ. The system operates at the KrF excimer wavelength of 248.6 nm (photon energy $\hbar\omega=4.99$ eV), and has a bandwidth of 20 meV or 160 cm^{-1}. The FWHM pulse duration is typically 500 fs, and the produced radiation is linearly polarized. To focus the beam, a CaF_2 planoconvex lens was used with a focal length of $f=200$ mm. In order to avoid any nonlinear absorption, the material of the entrance as well as the exit window is CaF_2. The amplified spontaneous emission (ASE) to pulse contrast ratio at focus is better than 10^{-6}. To attenuate the laser beam, a pair of dielectric plates with an angle-dependent attenuation covering three orders of magnitude, has been used. By rotating the plates over equal but opposite angles, the displacement of the beam caused by the first plate is exactly compensated for by the second. The pulse energy E_p was measured using a pyroelectric detector. Energy measurements were performed by averaging over at least ten laser pulses immediately before and after each ion yield measurement. The change of the transmission of the windows due to deposition of the evaporated magnesium or indium atoms has been taken into account by an additional measurement of the pulse energy after the exit window. The results have been corrected for the change of the window transmission. What is plotted in the following is the measured ion yields as a function of I_{av}, where the average intensity is given by [8]: $I_{\mathrm{av}}=I_0[f^2/(d^2-b^2)]$, where I_0 is the unfocused peak intensity (in $\mathrm{W\,cm}^{-2}$), f is the focal length of the lens, $d=10-15$ mm the distance between the focus and the center of the rectangular source volume, and $2b=1.8$ mm the size of the volume along the laser propagation direction. The unfocused intensity I_0 is determined using $I_0=E_p/(A_0\Delta t)$, where $A_0=10\times27\,\mathrm{mm}^2$ is the area of the unfocused beam normal to the beam direction, and $\Delta t=532.2$ fs is the width of the rectangular pulse profile that has the same energy as a Gaussian pulse profile with a FWHM of 500 fs. The laser beam entered the vacuum chamber that was kept at less than 10^{-7} mbar. It should be noted that the optical components of the attenuator, the lens and the window, caused an intensity-dependent spectral broadening of the laser radiation. Thus for the intensities used in the experiment the maximum spectral FWHM has been measured to be of the order of 850 cm^{-1} or 100 meV. Increased bandwidth may play a role in measurements like those presented in this work, in particular with respect to the resonant or nonresonant character of the ionization; no temporal broadening has been observed due to the propagation through these optical elements.

Sputtering occurred with Ar ions, produced by a sputtering gun (Leybold IQE 12/38) and mass selected by a Wien filter. Both are mounted at an angle of 45° with respect to the target surface. The primary ion acceleration voltage was typically 5 kV and the typical primary ion currents were 1 μA.

In the second version of ''atomization,'' a small ''homemade'' oven containing the metal under investigation has been used. The oven was operated at maximum 800 °C as measured by a thermocouple. An effusive atomic beam was expanding through a small aperture of 1 mm diameter, into the acceleration region of the TOF spectrometer. The side of the oven including the aperture was also serving as the repeller electrode of the spectrometer.

Ions created via laser postionization were pushed by a repeller voltage of about 1.5 kV towards the ion spectrometer entrance slit. This four-grid reflection (TOF) spectrometer [10–12] is capable of extracting ions from the well-defined confined volume in which ionization is eventually fully saturated. In this way, volume effects can be avoided. Laser polarization, propagation direction and spectrometer axis were at 90° to each other. In the present work the focal spot did not overlap with the confined source volume of the spectrometer. Instead we used the expanding part of the laser beam (behind the focal spot). In this way the spatial intensity dependence over the confined source volume is minimized. As a result of well-known spherical aberration effects the spatial intensity distribution is more homogeneous behind the focal spot than in front of it. Typical distances between the focal spot and the heart of the source volume are 10 to 15 mm. Further operational details of the spectrometer can be found elsewhere [14].

After flying through the spectrometer, the ions were detected using a double multichannel plate detector, a preamplifier and a 1 GHz digitizing oscilloscope (LeCroy 9384M). Raw data were stored in a PC where they were further processed.

NUMERICAL CALCULATIONS

The generalized two-photon ionization cross sections for Mg and Zn have been calculated in the following way. A full CI calculation was performed for the two valence electrons. For this purpose two-electron configurations were constructed from the corresponding ionic orbitals describing Mg^+ and Zn^+. Those orbitals were obtained from solving the corresponding effective one-electron Hamiltonian in a basis of *B* splines. The core electrons were described differently for the two atoms. In the case of Mg, a Hartree–Fock calculation was performed. Afterwards, a core polarization potential was added to the obtained Hartree–Fock potential, and a diagonalization of the resulting effective Hamiltonian gave the ionic orbitals used in the CI calculation for the valence electrons. For Zn, a quasirelativistic energy-consistent *ab initio* pseudo potential replaced all 28 core electrons. Again, a core-polarization potential was added to the effective one- and two-electron Hamiltonian operators used to obtain the ionic orbitals and the final Zn (valence) wave functions. The parameters for the pseudopotential and the core polarization potential were taken from Schautz *et al.* [19]. The calculations for Mg are fully nonrelativistic, while in the case of Zn, relativistic effects were partly included via the pseudo potential. For both atoms calculations of the cross sections were performed in length and velocity gauge. When the length gauge was used, the dipole operator was modified to take into account the influence of the core-polarization potential (see, e.g., [20]), but the corrections due to this effect were found to be small. A more detailed description of the calculational procedure for obtaining generalized multiphoton ionization cross sections using a valence-electron CI approach in a *B*-spline basis can be found in [21].

While no efforts were made to improve on the core polarization or pseudopotentials, it was carefully checked that convergence with respect to the *B*-spline basis and the number of configurations included in the CI calculations has been achieved. Converged results were obtained using 602 *B* splines of order 9 covering the radial variable from 0 to 300 a.u. The CI calculations were well converged when adopting about 2000 to 3000 configurations per quantum number of total angular momentum *L*. Due to the finite sphere (with radius 300 a.u.) covered by the *B* splines the electronic continuum is box discretized. The normalization factors used to go from the L^2 discretized continuum to the energy-normalized one were evaluated both using the density of states and a matching to phase-shifted Coulomb waves (see, e.g., [21]). A very close agreement between the normalization factors obtained by those two methods was obtained.

There are many references for energy levels and oscillator-strength values for Mg (see [22,23] and references therein). Those data are well reproduced in the present calculation. The same is true for the one-photon ionization spectrum. There exist even some theoretical two-photon ionization spectra by Moccia and Spizzo [24], Chang and Tang [25], and Mengali and Moccia [22,23]. The present calculations reproduce especially the two more recent calculations very accurately in shape (including the resonant structures due to one-photon resonances or autoionizing states) and, as far as this can be judged from the corresponding graphs, also good quantitative agreement is found. The situation is quite different for Zn. In this case, only energy levels are frequently reported in literature and a compilation can for example be found in the NIST tables [26]. Only a limited number of oscillator-strength values are given in the literature. To the authors' knowledge, there is no report of a previous theoretical or experimental study of the two-photon ionization spectrum of Zn.

The present calculation reproduces the energy levels of the lowest lying bound states of Zn as reported in literature (NIST tables [26]) for all angular momenta relevant to the present study. This is also the case for the corresponding ionization thresholds. The oscillator strength values for the transitions $4s^2\ ^1S \rightarrow 4s4p\ ^1P^0$, $4s4p\ ^1P^0 \rightarrow 4s5s\ ^1S$, and $4s4p\ ^1P^0 \rightarrow 4s4d\ ^1D$ agree reasonably well, i.e., within at least 30%, with the values reported in literature ([27,28], and references therein). An exception is the $4s4p\ ^1P^0 \rightarrow 4s5d\ ^1D$ transition, where the oscillator-strength value found in the present work is three orders of magnitude larger than the one given by Biemont and Godefroid [28], the latter being, however, very small. (In addition, the value given by those authors varies by four to five orders of magnitude when using either Hartree–Fock or multiconfiguration Hartree–Fock, our result lying in between those values.) The one-photon ionization spectrum shows good qualitative agreement with the experimental [29] and theoretical [30] spectra, but its magnitude is roughly a factor of 2 to 4 off (the theoretical spectrum given in literature is about a factor 2 larger than the experimental one, and the present calculation is about another factor 2 larger). Of course, using the present model where all core electrons are described by a pseudopotential, the one-photon ionization spectrum can only be evaluated up to a photon energy of about 11 eV, since above that energy the first dipole-allowed transition involving an inner-shell excitation ($3d^9 4s\ 2^2 4p$) appears. In fact, this state leads to a very prominent peak in the spectrum and is thus connected to the electronic ground state by a rather large transition dipole moment. The same limitation applied to the two-photon case restricts the energy range in which the present approach can describe the physical spectrum to photon energies below approximately 5.5 eV. In Fig. 1 the two-photon ionization spectrum of Zn is shown. Figure 1(a) shows the separate contributions from final states with *S* and *D* symmetry, respectively. Clearly, the total spectrum (shown in Fig. 1(b) for the two gauges) is dominated by the contribution from final states with *D* symmetry. In the case of all the two-valence-electron systems He [31], Mg [23–25], Zn (this work), and H_2 (Δ symmetry [32]) this appears to be the case close to the (two-photon) ionization threshold. It is also interesting to note that for all those systems the spectrum corresponding to final states with $S\ (\Sigma)$ symmetry show a minimum close to the ionization threshold that is

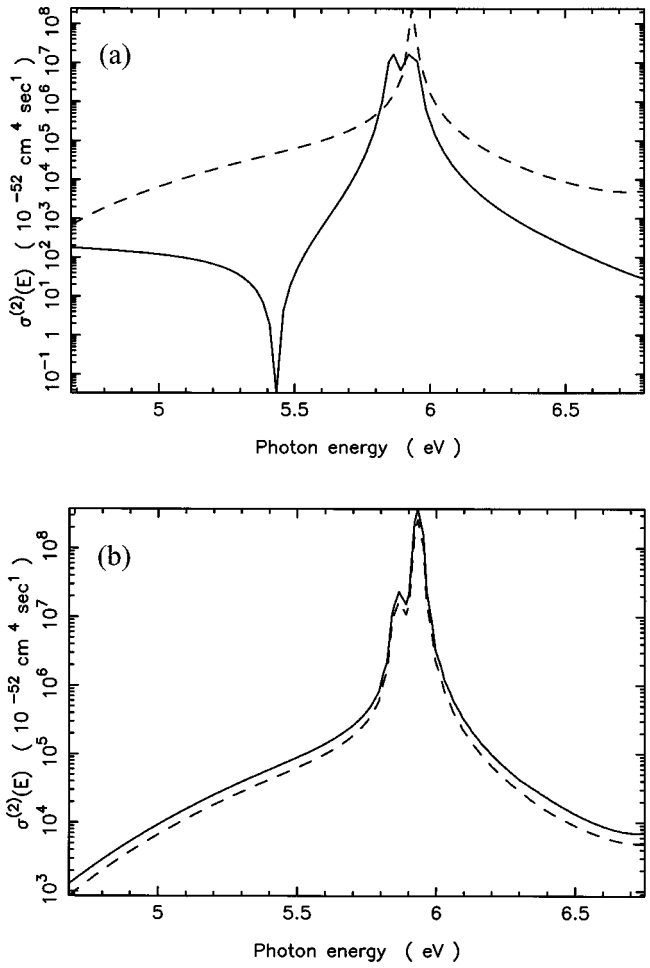

FIG. 1. Calculated two-photon ionization spectrum of Zn contributions from final states with *S* (solid line) and *D* (dashed line) symmetry (a); total spectrum calculated in the length (solid line) and velocity gauge (dashed line) (b).

caused by an interference of terms appearing in the summation over (virtual) intermediate states.

When comparing the absolute value of the generalized two-photon cross section of Zn with the experimental result, it is important to keep in mind the possible limitations of the present numerical approach. Relativistic effects, especially spin-orbit coupling, were not explicitly considered for the valence electrons. This is motivated by the fact that the dipole transitions from the ground state to bound triplet states are very small (see, e.g., [33]), but this may not be true for other transitions that should be considered in the summation over virtual intermediate states. The ability of the used core polarization and pseudopotential for reproducing oscillator-strength values may be limited (the potential was optimized to represent energy levels as accurately as possible), but again the (few) oscillator-strength values that could be compared with seem to indicate that the numerical approach is reasonable. Finally, the present approach completely ignores core-excited states. Also this is not expected to be a severe limitation for the photon energies considered, since the detuning of the photon from a one-photon resonance with such a state is more than 6 eV (and thus larger than the photon energy itself), but if the dipole moments are very large (and if sufficiently many of them contribute), those states may play some role. A final judgment on this issue would require a calculation that also includes those states explicitly. In conclusion, well-motivated approximations were used in the present numerical study, but the final judgment on their validity requires further theoretical and experimental studies. In this context, it would be very interesting to experimentally investigate the dependence of the Zn two-photon ionization cross section on the photon energy.

RESULTS

The atomic systems that have been experimentally investigated are ^{12}Mg (group II A), ^{30}Zn (group II B), and ^{49}In (group III B). These metals have ionization thresholds 7.646, 9.394, and 5.786 eV, respectively. Thus they undergo a two-photon ionization. The ground state configuration of Mg is $[\mathrm{Ne}]\,3s2\ ^1S$. The closest electric dipole allowed resonance, for the 4.99 eV photons of the experiment, is to the state $[\mathrm{Ne}]\ 3s3p\ ^1P^0$, with an excitation energy of 4.34 eV. Thus the detuning from this resonance is 650 meV and the process is expected to be nonresonant. The corresponding states for Zn are: $[\mathrm{Ar}]3d^{10}4s^2\ ^1S$ (ground state) and $[\mathrm{Ar}]3d^{10}4s4p\ ^1P$ (first dipole allowed resonance at 5.79 eV). The detuning is 806 meV, even larger than for Mg. For In we have a $[\mathrm{Kr}]\ 4d^{10}5s^25p\ ^2P$ ground state and the closest dipole allowed resonance, the $[\mathrm{Kr}]\ 4d^{10}5s^26d\ ^2D$ state, is at 4.84 eV and thus the detuning reads 160 meV. For this element a nearly resonant process cannot be excluded.

For these three elements the measured ion-yield versus laser-intensity curves for ions originating from the confined volume are shown in Figs. 2(a), 2(b), and 2(c). The full squares correspond to data obtained from atoms sputtered from solid targets, while the hollow circles are the results of evaporated atoms. For all three elements, saturation has been reached for the intensities used. The solid lines are fits of the expression: $CP(I,t\rightarrow\infty)$, where C is a constant used because the measured yields are in arbitrary units and $P(I,t\rightarrow\infty)=1-e^{-(I/I_{\mathrm{SAT}})^n}$, is the ionization probability (after the laser pulse is over) as a function of the laser intensity, which is the solution of population rate equations for a nonresonant n-photon ionization [14] and I_{SAT} the ionization saturation intensity as defined in, e.g., [14]. At low intensities this expression reduces to $P(I,t\rightarrow\infty)\approx(I/I_{\mathrm{SAT}})^n$, which in a log–log representation is a straight line with slope n. C and I_{SAT} are fit parameters. The parameter n should be equal to two for a nonresonant two-photon ionization process. It is kept though as a fit parameter in order to examine whether the process is indeed a pure two-photon ionization process, described by a single two-photon ionization rate, or possibly initially populated excited states give rise to deviations from this value, adding some single photon ionization character into the process. Once I_{SAT} and n are determined through the fit the generalized cross section can be extracted in a straightforward manner, as it is a function of these two parameters, the photon energy and the effective pulse duration [14]. Dashed lines are fits of the expression

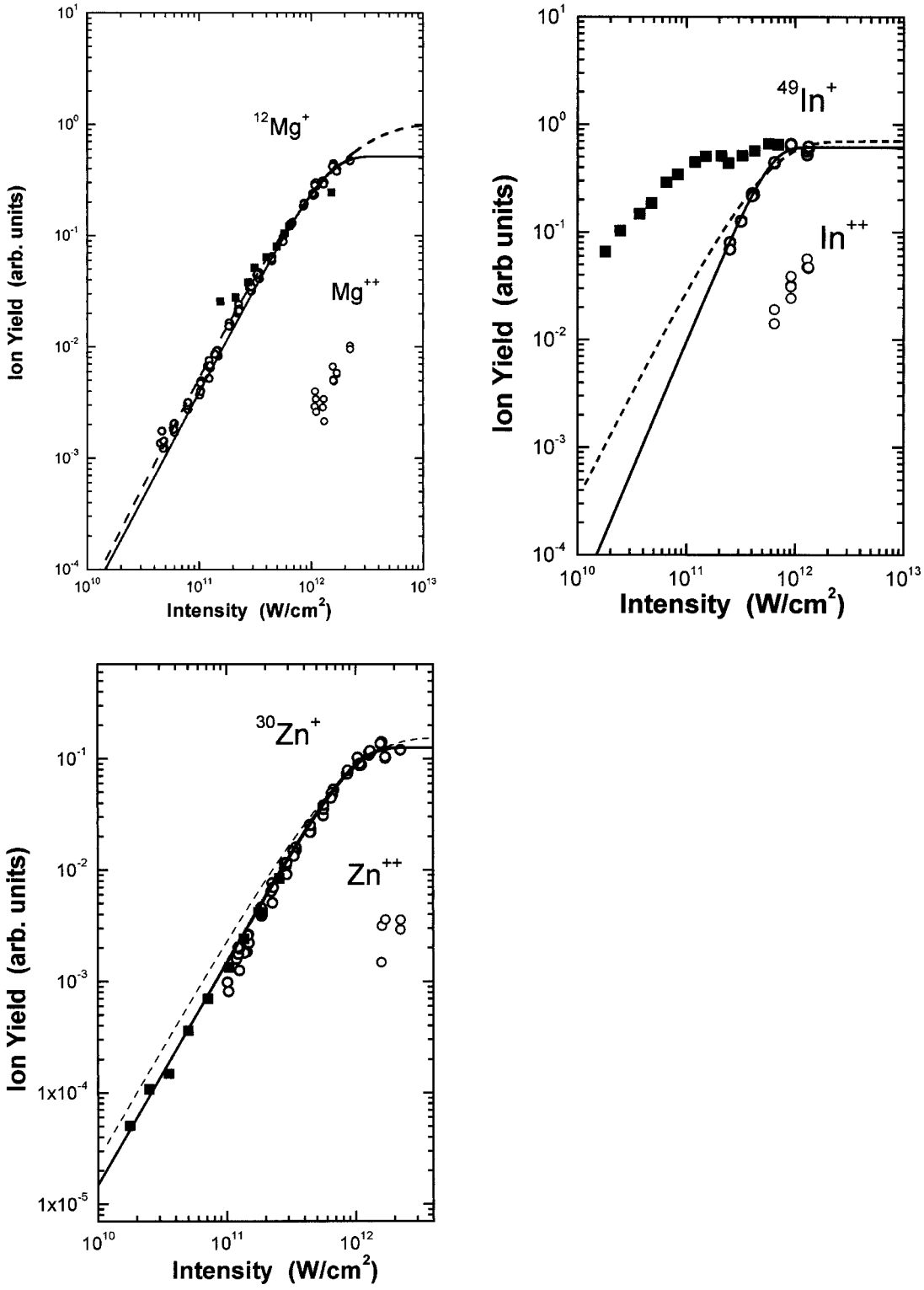

FIG. 2. Measured ion yield as a function of the laser intensity for: Mg $[Z=12]$ (a); Zn $[Z=30]$ (b); and In $[Z=49]$ (c). Solid lines are fits of the expression that describe an n-photon nonresonant ionization process, as explained in the text, with fit parameters the constant C, the ionization saturation intensity I_{SAT}, and the number of ionizing photons n. Dash lines are fits of the expression that describe a near resonant two-photon ionization process, as described in the text, with fit parameters the constant C' and the cross sections σ_1, σ_2.

$$P(\Phi) = C'\{1 + \tfrac{1}{2}[\sec(B-1)]e^{-(A/2)[\cos(B+1)]} - \tfrac{1}{2}[\sec(B+1)]e^{+(A/2)[\cos(B-1)]}\}$$

which is the solution of population rate equations for a resonant two-photon ionization [14], with C' a constant used because the measured yields are in arbitrary units, $A=[k+(2\sigma_1+\sigma_2)\Phi]\tau$ and $B=\arcsin(2\sqrt{\sigma_1\sigma_2}\Phi\tau/A)$, where Φ

TABLE I. Measured two-photon ionization saturation intensities and generalized cross section of Mg, Zn, and In at the wavelength of 248 nm and 500 fs pulse duration and the corresponding calculated two-photon generalized cross section for Mg and Zn.

	$\sigma^{(2)}_{\mathrm{EXPT}}(10^{-48}\,\mathrm{cm}^4\,\mathrm{s})$	$I_{\mathrm{SAT}}(10^{12}\,\mathrm{W/cm}^2)$	$\sigma^{(2)}_{\mathrm{TH}}(10^{-48}\,\mathrm{cm}^4\,\mathrm{s})$
^{12}Mg	1.1 ± 0.2	1.3 ± 0.2	1.0
^{30}Zn	2 ± 1	0.95 ± 0.3	0.9
^{49}In	5.2 ± 0.5	0.58 ± 0.03	

is the photon flux, σ_1,σ_2 the cross sections of the two absorption steps and k the decay rate of the intermediate resonance [14]. It should be noted that for a near resonant ionization process the product $k\tau$ becomes negligible [14] and thus knowledge of k is redundant. Fit parameters are the constant C' and the cross sections σ_1,σ_2. For Zn and In the expression describing a nonresonant process, with a slope very close to two, gives a much better fit than the expression describing a near resonant process, stating conclusively that the ionization process is, as expected, a two photon nonresonant one. For Mg both expressions for both resonant and nonresonant two-photon ionization give fits of similar quality. Thus the type of ionization of Mg is not distinguishable from the fitting procedure. There is though no definite evidence why this process should be a resonant one. The pulse bandwidth of the laser including the bandwidth broadening of 100 meV, mentioned in the experimental section, occurring through nonlinear effects at the different optical elements is not sufficient to support arguments for a resonant process in Mg. This is because the detuning from a one-photon resonance is similar to that in Zn and four times larger than in In. The resulting two-photon generalized cross sections and ionization saturation intensities for the ionization of the evaporated atoms are shown in Table I. The errors quoted are errors given by the fit. For Mg and Zn in Table I, the calculated two-photon ionization generalized cross sections are included. The agreement for Mg is excellent and for Zn is reasonable given the limitations described in the previous section and the experimental uncertainties in determining the laser intensity at the focus and in keeping the atomic number density constant.

Comparing the measured curves of sputtered (solid squares in Fig. 2) and evaporated atoms (hollow circles in Fig. 2), an unambiguous difference is observed in In. While the slope of the log–log curve for the ions produced from evaporated atoms is close to 2, its value in the case of sputtered atoms is 1.2. Saturation of ionization of sputtered atoms occurs at lower intensities than for evaporated atoms. These observations give strong evidence that the sputtering process creates a large percentage of atoms in excited states that photoionize through one-photon absorption. A reduction of the slope in the curve of the sputtered atoms is also observed for Mg. Because of the missing saturation plateau, we cannot extract a value for the saturation intensity. A single-photon ionization of excited states populated during the sputtering process of Mg cannot be excluded. In Zn, both curves of evaporated and sputtered atoms have the same slope of 2, which is compatible with a two-photon ionization. This observation alone cannot exclude the presence of population in excited states of sputtered Zn atoms. The first Zn excited state ($^3P^0$) is at 4 eV and thus its ionization with 4.99 eV photons is a two-photon process as is the ionization of the ground state too. One would of course expect two different cross sections and consequently two different ionization rates and saturations intensities. This has not been observed in the present measured.

For all three metals, double ionization has also been observed with an appearance intensity close to the single ionization saturation intensity.

CONCLUSIONS

The experimental set-up using the evaporating technique that has been developed and used in our experiments has proven to be an efficient tool for quantitative measurements of the multiphoton-ionization probability. We have thus measured the two-photon generalized ionization cross sections for Mg, Zn, and In. By means of a full valence CI calculation, theoretical two-photon ionization cross sections of Mg and Zn were obtained and compared with the experimental ones. The measured values for Mg and Zn have been in reasonable agreement with the calculated theoretical ones. Previous experiments using sputtering have shown that atoms produced in excited states complicate the quantification of the experimental results. This effect was clearly absent using the evaporating technique. The comparative study of both methods' results for the metals Mg, Zn, and In showed that the role of atoms produced in excited states is important in the case of In but minor in the case of Zn. This verifies that the importance of excited atoms produced during the sputtering process is element specific. No general conclusions can be drawn and each element has to be separately studied in this respect.

Finally, the curves measured using the evaporating technique are more accurate in describing multiphoton processes than the ones measured in previous experiments using the sputtering technique. In case the melting of the sample is not a problem, the evaporating technique not only provides useful information on the nature of multiphoton processes, but also on the effects of the sputtering technique.

ACKNOWLEDGMENTS

This work was carried out in the Ultraviolet Laser Facility (ULF) operating at FORTH-IESL (TMR Contract No. ERB-FMGE-CT950021) and was partially supported by the ΕΠΕΑΚ program of the Greek Ministry of Education. We would like to thank A. Eglezis for his skillful technical assistance.

[1] G. Voronov and N. Delone, JETP Lett. **1**, 66 (1965); P. Agostini, G. Barjot, J. F. Bonnal, G. Mainfray, and C. Manus, IEEE J. Quantum Electron. **QE-4**, 667 (1968).
[2] For SNMS, see, e.g., H. Oechsner, Nucl. Instrum. Methods Phys. Res. B **33**, 918 (1988).
[3] C. H. Becker and K. T. Gillen, Anal. Chem. **56**, 1671 (1984); B. Witzel, H. Schröder, S. Kaesdorf, and K.-L. Kompa, Int. J. Mass Spectrom. Ion Processes **172**, 229 (1998).
[4] M. Miyabe, M. Oba, and I. Wakaida, J. Phys. B **33**, 4957 (2000).
[5] S. Speiser and J. Jortner, Chem. Phys. Lett. **44**, 399 (1976).
[6] S. Kaesdorf, M. Hartmann, H. Schröder, and K.-L. Kompa, Int. J. Mass Spectrom. Ion Processes **116**, 219 (1992).
[7] M. Cerveman and N. Isenor, Opt. Commun. **13**, 175 (1975).
[8] P. Hansch and L. van Woerkom, Opt. Lett. **21**, 1286 (1996).
[9] M. A. Walker, P. Hansch, and L. D. Van Woerkom, Phys. Rev. A **57**, R701 (1998).
[10] M. Wagner and H. Schröder, Int. J. Mass Spectrom. Ion Processes **128**, 31 (1993).
[11] H. Schröder, M. Wagner, S. Kaesdorf, and K.-L. Kompa, Ber. Bunsenges. Phys. Chem. **97**, 1688 (1993).
[12] H. Schröder, M. Wagner, and S. Kaesdorf, *Material Analysis based on Quantitative Laser Ionization*, Excimer Lasers, edited by L. D. Laude (Kluwer Academic, Boston, 1994).
[13] E. Krishnahmer, S. A. Ranwala, and S. K. Mitra, J. Phys. B **29**, L657 (1996).
[14] B. Witzel, C. J. G. J. Uiterwaal, H. Schröder, D. Charalambidis, and K.-L. Kompa, Phys. Rev. A **58**, 3836 (1998).
[15] B. Witzel, N. A. Papadogiannis, C. J. G. J. Uiterwaal, H. Schröder, and D. Charalambidis, Phys. Rev. A **60**, 3311 (1999).
[16] G. Betz and K. Wien, Int. J. Mass Spectrom. Ion Processes **140**, 1 (1994), and references therein.
[17] S. Szatmári and F. P. Schäfer, Opt. Commun. **68**, 196 (1988).
[18] P. Simon, H. Gerhardt, and S. Szatmári, Opt. Commun. **71**, 305 (1989).
[19] Schautz, H.-J. Flad, and M. Dolg, Theor. Chem. Acc. **99**, 231 (1998).
[20] P. Hafner and W. H. E. Schwarz, J. Phys. B **17**, 2975 (1978).
[21] P. Lambropoulos, P. Maragakis, and J. Zhang, Phys. Rep. **305**, 203 (1998).
[22] S. Mengali and R. Moccia, J. Phys. B **29**, 1597 (1996).
[23] S. Mengali and R. Moccia, J. Phys. B **29**, 1613 (1996).
[24] R. Moccia and P. Spizzo, J. Phys. B **21**, 1145 (1988).
[25] T. N. Chang and X. Tang, Phys. Rev. A **46**, R2209 (1992).
[26] NIST tables of physical reference data: http://physics.nist.gov/PhysRefData/contents.html
[27] T. Brage and C. Froese Fischer, Phys. Scr. **45**, 43 (1992).
[28] E. Biemont and M. Godefroid, Phys. Scr. **22**, 231 (1980).
[29] G. V. Marr and J. M. Austin, J. Phys. B **2**, 107 (1969).
[30] M. Stener and P. Decleva, J. Phys. B **30**, 4481 (1997).
[31] A. Saenz and P. Lambropoulos, J. Phys. B **32**, 5629 (1999).
[32] A. Apalategui and A. Saenz (unpublished).
[33] J. Bruneau, J. Phys. B **17**, 3009 (1984).